Binding of Substrates to Human Deoxycytidine Kinase Studied with Ligand-Dependent Quenching of Enzyme Intrinsic Fluorescence†

Borys Kierdaszuk,‡,§,‖ Rudolf Rigler,*,‡ and Staffan Eriksson§

Department of Medical Biophysics and Medical Nobel Institute, Department of Biochemistry I, Karolinska Institute, Box 60400, S-104 01 Stockholm, Sweden, and Department of Biophysics, Institute of Experimental Physics, University of Warsaw, 93 Zwirki i Wigury Str., PL-02 089 Warsaw, Poland

Received June 1, 1992; Revised Manuscript Received September 17, 1992

ABSTRACT: Deoxycytidine kinase is a key enzyme in the salvage pathway, and its activity is required for 5′-phosphorylation of several important antiviral and cytostatic nucleoside analogues. It has recently been purified completely from human sources. Steady-state and time-resolved fluorescence of human deoxycytidine kinase was used to study its interaction with the substrates dCyd, dAdo, dUrd, dTTP, and the feedback inhibitor dCTP. Enzyme fluorescence quenching by dCTP, dCyd, dTTP, and dAdo was bimodal, and the best fits of the quenching patterns were obtained using two modified Stern–Volmer equations with two sets of quenching constants (K_{sv}) and accessibility values (f_a) fitted independently for "low" and "high" concentration ranges of ligands. The transition between these occurred at about 20 μM dCTP, 50 μM dCyd, 30 μM dTTP, and 180 μM dAdo. Enzyme fluorescence showed unimodal quenching by dAdo and 30% reduced accessibility of the binding site in the presence of dCyd. dUrd quenching was also unimodal with $K_{sv} = 0.0047 \pm 0.0007$ μM^{-1} and $f_a = 0.75 \pm 0.05$, hence in the same range as for the "high" concentration range of dAdo in the absence of dCyd, where they are 0.0025 ± 0.0003 μM^{-1} and 0.73 ± 0.03, respectively. Fluorescence quenching was used to directly determine enzyme–ligand binding and revealed bimodal binding of dCTP, dCyd, dTTP, and dAdo and unimodal binding of dUrd, and of dAdo in the presence of 0.1 μM dCyd. Transition between these two modes of binding occurred at the concentrations described above. At the high concentration range of ligands, binding is characterized by 1–2 order of magnitude lower association constants than at the low concentration range, and severalfold higher binding capacities. Stoichiometry calculation gives about 1 molecule of ligand bound per 61-kDa dimer enzyme, except for dCTP, where it is equal to 0.6 ± 0.2. The transition between the native and the unfolded form of the enzyme showed a midpoint of unfolding equal to 3.2 M guanidine hydrochloride, and after denaturation, the emission peak was shifted from 332 to 350 nm, the excitation peak remained unchanged at 285 nm, and the fluorescence quantum yield had decreased 2-fold. High-resolution photon counting gave fluorescence lifetimes ranging from tens of picoseconds to 10 ns with the best nonlinear least-squares fits corresponding to a sum of four discrete exponential terms. Static quenching of three excited states and dynamic quenching of one excited state were observed on interaction with dCyd. The fluorescence anisotropy decays are typical for this size class of enzymes and suggest that human deoxycytidine kinase has a relatively rigid structure. Interaction with 10 μM dCyd did not affect the motion of tryptophans and did not lead to aggregation of the enzyme subunits. Several models to explain the binding properties of human deoxycytidine kinase are described.

Deoxycytidine kinase (dCyd kinase)[1] (NTP:deoxycytidine-5′-phosphotransferase, EC 2:7.1.74) catalyzes the phosphorylation of 2′-deoxycytidine (dCyd) to 2′-deoxycytidine 5′-monophosphate (dCMP) in the presence of a nucleoside 5′-triphosphate phosphate donor. The cytosolic enzyme has been isolated and partially purified from many sources (Kessel, 1968; Momparlier & Fisher, 1968; Durham & Ives, 1970a,b; Kazai & Sugino, 1971; Coleman et al., 1975; Krenitsky et al., 1976; Cheng et al., 1977; Meyers & Kreis, 1976; Hurley et al., 1983; Sarup & Fridland, 1987; Datta et al., 1989). dCyd kinase has been purified to apparent homogeneity from human leukemic spleen (Bohman & Eriksson, 1988) and leukemic human T-lymphoblasts (Kim et al., 1988). Most investigators have found that the same enzyme also phosphorylated purine deoxyribonucleosides including several nucleoside analogues (Krenitsky et al., 1976; Eriksson et al., 1991a; Kierdaszuk et al., 1992). Recently, it was shown that human enzyme (Eriksson et al., 1991a) is able to phosphorylate Cyd, dUrd, and Thd but with an enzyme efficacy 20-, 10^3-, and 10^4-fold lower than for dCyd.

The cDNA coding for human dCyd kinase has been cloned by Chottiner et al. (1991), and the cloned enzyme expressed in *Escherichia coli* had a subunit molecular mass of 30.5 kDa and a substrate specificity similar to the enzyme from human spleen. The peptide sequences (Eriksson et al., 1991b) of the pure spleen enzyme demonstrated that the cloned cDNA (Chottiner et al., 1991) coded for this enzyme while an earlier

† This work was supported by grants from the Swedish Medical Research Council, the Swedish Natural Science Research Council, the Swedish Cancer Society, the Medical Faculty of the Karolinska Institute, and by KBN through the Polish Ministry of National Education (Project 4 1514 91 01).

* Address correspondence to this author at the Medical Nobel Institute, Department of Biochemistry I, Karolinska Institute, Box 60400, S-104 01 Stockholm, Sweden.

‡ Department of Medical Biophysics, Karolinska Institute.

§ Department of Biochemistry, Karolinska Institute.

‖ Department of Biophysics, University of Warsaw.

[1] Abbreviations: dCyd kinase, deoxycytidine kinase; BSA, bovine serum albumin; CHAPS, 3-[(3-cholamidopropyl)dimethylammonio]-1-propanesulfonate; DTT, dithiothreitol; Tris-HCl, tris(hydroxymethyl)-aminomethane hydrochloride; Gdn-HCl, guanidine hydrochloride; dCyd, dAdo, dGuo, Thd, and dUrD, 2′-deoxyribonucleosides of cytosine, adenine, guanine, thymine, and uracil, respectively; NTP, nucleoside triphosphate; dNTP, 2′-deoxynucleoside triphosphate.

0006-2960/93/0432-699$04.00/0

described cDNA (Huang et al., 1989) coded for another unrelated protein.

Previous studies have shown that the kinetic behavior of dCyd kinase is very complex and that the enzyme exhibits negative cooperativity with ATP as the phosphate donor (Ives & Durham, 1970; Bohman & Eriksson, 1988), and with dCyd, ara-C, and dAdo as phosphate acceptors (Ives & Durham, 1970; Sarup & Fridland, 1987; Kierdaszuk & Eriksson, 1990; Bohman et al., 1992). However, the molecular mechanism of this phenomenon is not clear, and therefore we have used ligand-dependent enzyme fluorescence to get more information about the interaction between the enzyme and its substrates and inhibitors. There are 7 tryptophans and 12 tyrosines per 30.5-kDa subunit, which is a source of enzyme fluorescence.

We studied the effect of binding of substrates (dCyd, dAdo, dUrd, and dTTP) and feedback inhibitor (dCTP) to dCyd kinase by determining the response of its fluorescence to increasing concentration of ligand. The enzyme–ligand interaction is accompanied by a partial quenching of the enzyme fluorescence and therefore permits its use as an experimental tool. The results presented in this paper show that the bimodal kinetics of this enzyme are apparently reflected by the enzyme–ligand interaction.

MATERIALS AND METHODS

Materials. [5-^{3}H]-2′-Deoxycytidine (19.3 Ci/mmol) and [G-^{3}H]-2′-deoxyadenosine (29 Ci/mmol) were purchased from the Radiochemical Center, Amersham, U.K. Unlabeled nucleosides, guanidine hydrochloride, and ATP (disodium salt) were obtained from Sigma Chemical Co., and dTTP (trisodium salt) was from Pharmacia Inc. (Molecular Biology Division). The zwitterionic detergent 3-[(3-cholamidopropyl)dimethylammonio]-1-propanesulfonate (CHAPS) was purchased from Boehringer Mannheim.

The TSK-G3000SW column and the Superose 12,HR 10/30 (300 × 10 mm) column were purchased from Pharmacia LKB Biotechnology, Sweden. The calibration proteins, size I, for column calibration were from Boehringer Mannheim. All other chemicals, reagents, and materials were of the highest quality commercially available, and only those with a spectral-grade quality, checked by UV absorption and/or fluorescence measurements, were used.

Preparation and Characterization of dCyd Kinase. dCyd kinase was purified from human leukemic spleen by streptomycin sulfate precipitation, fractionated ammonium sulfate precipitation, DEAE ion-exchange chromatography, hydroxylapatite chromatography, and affinity chromatography on dTTP–Sepharose as described by Bohman and Eriksson (1988). In order to concentrate the enzyme after affinity chromatography and remove dTTP, we have used a second hydroxylapatite column (7 × 10 mm), which was equilibrated with 10 mM potassium phosphate buffer (pH 7.6) containing 5 mM $MgCl_2$, 20% glycerol, and 1 mM DTT (buffer A). After dTTP–Sepharose chromatography, fractions containing dCyd kinase activity were pooled and applied to the hydroxylapatite column. The column was washed with 20–50 column volumes of buffer A until there was no dTTP present in the eluate, as detected by UV absorbency. dCyd kinase was eluted with buffer A containing 0.2 M phosphate buffer (pH 7.6), and 0.2–0.5-mL fractions of concentrated enzyme (100–300 mg/mL) were collected. Enzyme activity was measured with 10 μM dCyd as phosphate acceptor and 1 mM ATP as phosphate donor (Kierdaszuk & Eriksson, 1990). Protein was determined with the Bradford method (Bradford, 1976), and the concentration of pure enzyme was quantitated by amino acid analysis (Eriksson et al., 1991). The enzyme was purified about 10^4-fold to near-homogeneity and had a specific activity of about 150 nmol min^{-1} (mg of protein)$^{-1}$ at 10 μM dCyd. The purity of the enzyme was determined using SDS–polyacrylamide gel electrophoresis (O'Farrel, 1975) and analytical gel filtration chromatography (Kierdaszuk & Eriksson, 1990; see also below). The polypeptide bands were visualized by positive-image silver staining (Merril et al., 1984). Due to the high concentration of protein and the stabilizing effect of ligands (Kierdaszuk & Eriksson, 1990), the specific activity of dCyd kinase was not affected by titration with dCyd, dAdo, and dTTP as checked by activity measurement before and after the experiments.

Analytical gel filtration chromatography was performed by HPLC on a TSK-G3000SW (600 × 7.5 mm) column (Kierdaszuk & Eriksson, 1990) and by FPLC (Parmacia, Sweden) on a Superose 12,HR 10/30 (300 × 10 mm) column with a single-path monitor UV-1 detector (Pharmacia) operating at 280 nm. The Superose column was equilibrated and eluted at a flow rate of 0.2 mL^{-1} min^{-1} $fraction^{-1}$ using 50 mM Tris-HCl (pH 7.6) buffer containing 5 mM $MgCl_2$, 0.1 M KCl, and 1 mM DTT. Catalase (M_r 240 000), BSA (M_r 67 000), ovalbumin (M_r 43 000), and chymotrypsinogen A (M_r 25 000) were used as molecular weight markers for column calibration. The elution volume of these standard proteins and dCyd kinase was determined by following their absorbency at 280 nm, dCyd kinase activity vs. dCyd and dAdo, and the polypeptide bands on SDS–polyacrylamide gel electrophoresis.

Steady-State Fluorescence Measurements. Absorption measurements were performed on Cary 118 and Beckman DU-50 spectrophotometers. Steady-state fluorescence spectra were measured at 20 °C on a Shimadzu RF-540 spectrofluorometer (with 2-nm spectral resolution for excitation and emission) using 0.5–1 μM solutions of pure dCyd kinase (see above) in 160–200 μL of 50 mM Tris-HCl (pH 7.6) containing 5 mM $MgCl_2$, 20% glycerol, and 1 mM DTT (buffer B) or in 0.2 M potassium phosphate buffer (pH 7.6) containing 5 mM $MgCl_2$, 20% glycerol, and 1 mM DTT (buffer C). Samples were placed in 4.4 × 4.4 mm Suprasil cuvettes for all spectral measurements. Protein fluorescence was excited at several wavelengths in the range 260–300 nm, and fluorescence spectra were recorded in the 280–450-nm range, while the changes of fluorescence were usually monitored at the emission maximum (332 nm).

For quenching studies, additions to the enzyme sample were made from quencher stock solutions prepared in the same buffer as the enzyme sample; dilution did not exceeded 10%, and in each experiment, the fluorescence intensity was corrected for the dilution factor. Background emission (<5%) was eliminated by subtracting the signal from buffer containing the appropriate quantity of ligand. To compensate for the decrease in fluorescence caused by increased absorption, the measured fluorescence was multiplied by a correction factor, $G(A,d) = \exp(d/2\Delta A)$, where d is the optical path length and ΔA is the increase of total absorption at the excitation wavelength when ligand was added (Ehrenberg et al., 1971). The total absorption of the enzyme sample did not exceed 0.1 at 285 nm.

The excitation–emission contour maps were measured using computer-aided scanning (Rigler et al., 1989) in the ranges 240–320 and 280–450 nm for excitation and emission wavelengths, respectively. After subtraction of background fluorescence, enzyme fluorescence spectra were plotted as a contour map against excitation and emission wavelengths

(Figure 1). For both wavelengths, the 2-nm step and 2-nm spectral slits were used.

Time-Resolved Fluorescence Measurements. Time-resolved single photon counting measurements of the fluorescence and fluorescence anisotropy were performed and analyzed as described elsewhere in detail (Rigler et al., 1985; Claesens & Rigler, 1986). The synchronously pumped (argon laser, 76 MHz), mode-locked, cavity-dumped (8 MHz) dye laser was tuned to 590 nm and frequency-doubled to 295 nm for efficient excitation of the tryptophan residues of dCyd kinase. The dye laser pulse full width at half-maximum was about 6 ps, as measured with an autocorrelator. The detection system was based upon a Hamamatsu microchannel plate photomultiplier (R1564U) set up in the time-correlated single photon counting mode. The overall system response time was 70 ps FWHM. Fluorescence excited by the vertical polarized pulse was collected by a suprasil lens and filtered through Schott WG320 (3 mm thick) and through a sheet polarizer. For each measurement, four data sets were collected: the laser pulse profile, the fluorescence with the emission polarizer set at the magic angle (54.7°), the dark current (laser beam blocked), and the fluorescence with the polarizer set horizontally (perpendicular to excitation polarization). The sets were collected in 1 min/set cycles. The cycle was repeated 10–20 times. Each set contained 2048 channels of data, with 1 channel corresponding to 26 ps. The fluorescence signal, free from polarization effects, is directly given by the magic angle signal, after subtraction of dark current. Anisotropy signals were calculated from magic and perpendicular fluorescence components. Determination of the time delay caused by the different optical path taken by the fluorescence light and the excitation light was made in two ways. First, the sample was replaced by a dilute suspension of glycogen from which scattered light was measured. The difference in position of the peak of this scattering and the peak of the excitation pulse measured in the normal way gave the relative time delay. Alternatively, the delay time was calculated by allowing the time delay to be a fitting parameter in some of the sample anisotropy decays. The two methods for determination of the time delay agreed to within one data channel. The delay was left fixed for all subsequent data fits. Accurate determination of this delay is important to obtain reliable anisotropy decays on the time scale of the system response time.

Fluorescence and anisotropy data were fitted to sums of exponentials, convoluted with the instrument response, by a least-squares fitting procedure (Marquardt, 1963). The quality of fit was evaluated by the structure observed in residuals plots and by the reduced χ^2 values:

$$\chi^2 = [1/(N-C)]\sum_{i=1}^{N}(e_i - f_i)^2/f_i$$

where N is the number of observed (e_i) and calculated (f_i) data points and C is the number of parameters in the model.

Analysis of the Steady-State Fluorescence Quenching Data. Analysis of fluorescence quenching data took into account three types of quenching mechanisms: dynamic quenching due to time-dependent diffusive collisions between fluorophore and quencher; static quenching as a result of formation of a nonfluorescent ground-state complex between the fluorophore and quencher; and combined dynamic and/or static quenching of fluorophores differing in accessibility to quencher. Each mechanism was described by a Stern–Volmer-type equation which relates the fractional decrease of enzyme fluorescence to the concentration of quenching ligand.

For dynamic quenching:

$$F_0/F = \tau_0/\tau = 1 + K_{SV}[L_0] \quad (1)$$

where F and F_0 are the fluorescence intensities in the presence and absence of a quenching ligand, respectively, τ and τ_0 are the fluoresence lifetimes in the absence and presence of quencher, respectively, and K_{SV} is the Stern–Volmer constant for dynamic quenching, equal to $k_q\tau_0$ where k_q is the bimolecular rate constant for the quenching process. The Stern–Volmer constant is a measure of the propensity of excited state(s) of fluorophores to quenching. Hence, a plot of F_0/F or τ_0/τ against $[L_0]$ should be linear for a homogeneous population of emitting fluorophores, when they are all equally accessible to the quenching ligand and subjected only to dynamic quenching (Eftink & Ghiron, 1981).

For static quenching, $\tau_0/\tau = 1$ and

$$F_0/F = 1 + K_S[L_0] \quad (2)$$

where K_S is the static quenching constant and is equal to the association constant for enzyme–ligand complex (Lakowicz, 1983).

Sometimes the fluorescence can be quenched both by collisional and by complex formation with the same quencher. In that case, the modified form of the Stern–Volmer equation for combined dynamic and static quenching was used (Lakowicz, 1983):

$$F_0/F = (1 + K_S[L_0])(1 + K_{SV}[L_0]) \quad (3)$$

Numerical fitting analysis (see below) revealed that eq 1–3 do not fit the experimental points. Therefore, a modified form of the Stern–Volmer equation was used to analyze the quenching of heterogeneous emitting fluorophores (Lehrer, 1971; Lehrer & Leavis, 1978):

$$F_0/(F_0 - F) = 1/([L_0]f_aK_{SV}) + 1/f_a \quad (4)$$

where f_a is the fractional accessibility, i.e., the maximum fraction of the protein fluorescence (tryptophan residues) accessible to quencher. A plot of $F_0/(F_0-F)$ vs $1/[L_0]$ should yield a straight line having a slope of $1/f_aK_{SV}$ and an intercept of $1/f_a$. We have fitted the nonlinear form of eq 4, $F([L_0])$, to the experimental data.

Equations 1–4 were fitted to the experimental data and the Stern–Volmer constants determined by nonlinear regression analysis, using an IBM PC computer and the Enzfitter program (Leatherbarrow, 1987, 1990) with the algorithm of Marquardt (1963). Equations 1–4 were fitted in the form of experimental data, $F([L_0])$, and eq 8 and 9 (see below) in the form of $V([L])$. The reduced χ^2 and residuals—the differences, and/or relative differences, between calculated values and experimental values—were used to test the quality of the fits.

Theoretical Model of Ligand Binding. The basic assumption of this model is that there is a linear relation between the fluorescence of free enzyme or enzyme–ligand complex and the enzyme or enzyme–ligand concentration, respectively. For this assumption to be valid, one needs to exclude an inner-filter effect of the absorbing species on the enzyme intrinsic fluorescence, and we used appropriate conditions to fulfill this requirement (see above).

For the elementary association step $E + L \rightleftharpoons EL$, there is a set of six equations with six unknown values (K, [E], [L], [EL], F_E, F_{EL}):

$$K = [EL]/[E][L] \quad (5.1)$$

$$F = [E]F_E + [EL]F_{EL} \quad (5.2)$$

$$[E_0] = [E] + [EL] \quad (5.3)$$

$$[L_0] = [L] + [EL] \quad (5.4)$$

$$F_0 = [E_0]F_E \quad (5.5)$$

$$F_i = [E_0]F_{EL} \quad (5.6)$$

where K is the intrinsic binding constant (an *association* constant) of the enzyme–ligand complex; [E], [L], and [EL], the molar concentration of free enzyme, free ligand, and enzyme–ligand complex, respectively; $[E_0]$ and $[L_0]$, the total concentrations of enzyme and ligand, respectively; F_E and F_{EL}, the fluorescence coefficients of free enzyme and enzyme–ligand complex, respectively; F_0, F, and F_i, the total fluorescence of the enzyme sample during titration at zero, intermediate, and saturated concentrations of ligand, respectively. Solving this set of equations results in

$$[L_0]/(F_0 - F) = 1/[K(F - F_i)] + [E_0]/(F_0 - F_i) \quad (6.1)$$

$$[E] = [E_0](F - F_i)/(F_0 - F_i) \quad (6.2)$$

$$[EL] = [E_0](F_0 - F)/(F_0 - F_i) \quad (6.3)$$

$$[L] = [L_0] - [E_0](F_0 - F)/(F_0 - F_i) \quad (6.4)$$

$$F_E = F_0/[E_0] \quad (6.5)$$

$$F_{EL} = F_i/[E_0] \quad (6.6)$$

It is worth noting that, when $[L_0] \gg [E_0]$, $[L_0] \gg [E_0](F_0 - F)/(F_0 - F_i)$ and eq 6.4 becomes $[L] \approx [L_0]$.

Using eq 6.3 and 6.4, analysis of the data can be done in the form of the Scatchard equation (1949):

$$V/[L] = K(N - V) \quad (7)$$

where N is the number of binding sites (binding capacity) for the ligand on each enzyme molecule; K, the intrinsic binding constant (an *association* constant) for each binding site; $V = (F_0 - F)/(F_0 - F_i)$, the number of moles of ligand bound per mole of total enzyme; [L], the molar concentration of free ligand.

Alternatively, eq 7 may be transformed into (Klotz & Hunston, 1971)

$$V = NK[L]/(1 + K[L]) \quad (8)$$

and for the two classes of binding sites (states) of enzyme characterized by different association constants (K_1, K_2) and binding capacities (N_1, N_2):

$$V = N_1K_1[L]/(1 + K_1[L]) + N_2K_2[L]/(1 + K_2[L]) \quad (9)$$

RESULTS AND DISCUSSION

Fluorescence Characteristics of dCyd Kinase in Native and Unfolded Forms. Fluorescence spectra of pure dCyd kinase were measured in buffer B (Materials and Methods) in the absence and presence of increasing concentrations of the denaturing agent Gdn-HCl, which provides information on

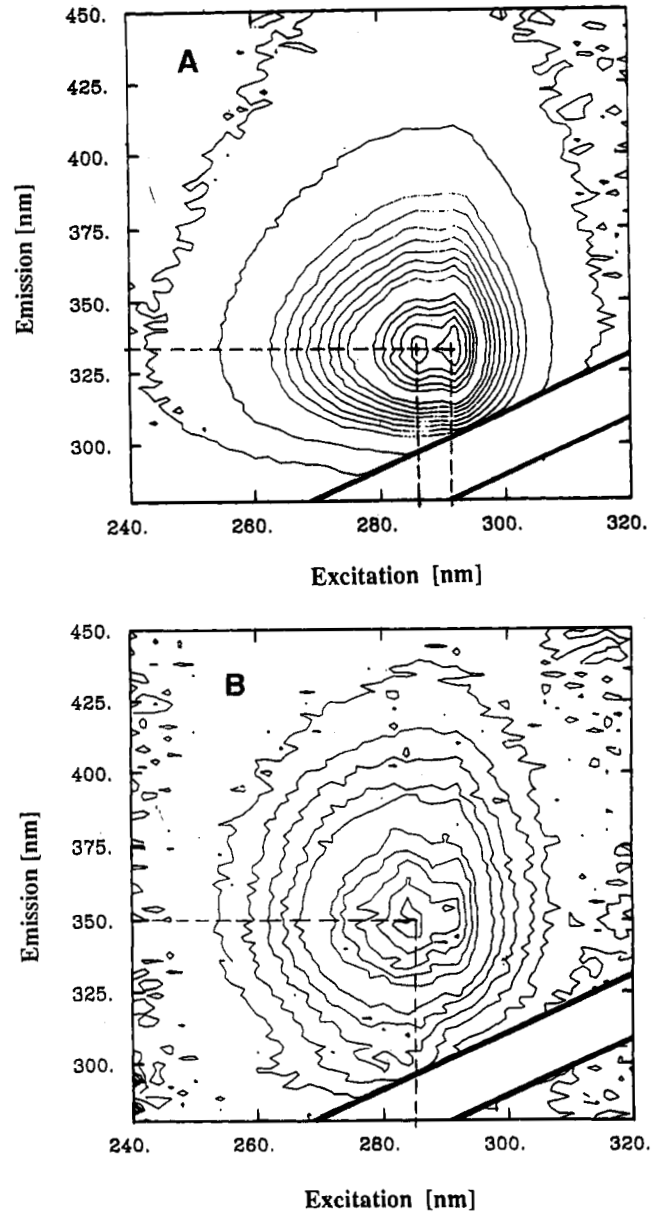

FIGURE 1: Excitation–emission contour maps of human dCyd kinase at 20 °C in buffer B (Materials and Methods) in the absence (A) and in the presence of 4.2 M Gdn-HCl (B). Contour lines represent iso-intensities normalized with respect to excitation-emission peaks.

the stability of the protein structure (Tanford, 1968) and the environment of the fluorophores (Lakowicz, 1983). In the absence of Gdn-HCl, the emission maximum was located at 332 nm and the excitation maximum at 287 nm, with a small side peak at 292 nm (Figure 1A). Hence, it was shifted to the red relative to the UV absorption maximum at 277 nm. Excitation–emission contour maps were measured in the absence (Figure 1A) and presence (Figure 1B) of 4.2 M Gdn-HCl. There was no change in the excitation–emission map when the Gdn-HCl concentration increased from 4.2 to 7.0 M. The titration of enzyme fluorescence with Gdn-HCl was recorded at seven excitation wavelengths (260, 265, 270, 280, 285, 290, and 295 nm) and one emission wavelength (332 nm). The same titration profiles (Figure 2) were obtained at all excitation wavelengths, indicating one unfolding process common for the entire protein molecule. Increasing the concentration of Gdn-HCl did not affect the position of the excitation band, but its substructure disappeared (Figure 1B). Unfolding of dCyd kinase was accompanied by a red shift of

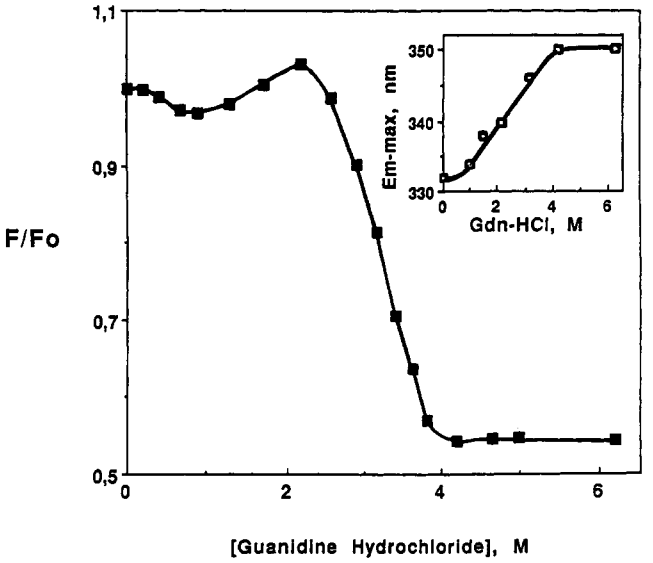

FIGURE 2: Effect of Gdn-HCl concentration on the fluorescence intensity of human dCyd kinase measured at 285-nm excitation and maximum emission wavelengths and expressed as a fraction of the unchanged fluorescence F_0. The insert shows the position of the emission peak at 285-nm excitation wavelength and different concentrations of Gdn-HCl. The fluorescence of 0.5 μM dCyd kinase in buffer B (Materials and Methods) was measured at 20 °C with addition of increasing concentrations of Gdn-HCl.

the emission band (Figure 1 and Figure 2, insert) and by a 2-fold decrease in fluorescence intensity (Figure 2). The fluorescence of the unfolded protein had a single peak in the excitation–emission contour map at 287-nm excitation and 350-nm emission (Figure 1B). The Gdn-HCl concentration at the midpoint of the transition curve was 3.2 M.

From the foregoing, we may conclude that human dCyd kinase has a typical tryptophanyl fluorescence. Its tryptophans are buried inside in a nonpolar environment of a relatively rigid protein structure (see also analysis of time-resolved spectra, below). Unfolding of dCyd kinase exposes these residues to the polar environment which shifts the emission maximum to the red.

Enzyme Fluorescence Quenching by dCTP, dTTP, dCyd, and dAdo. Kinetic results with dCyd kinase have shown biphasic saturation curves with dCyd and dAdo as substrate (Durham & Ives, 1970b; Ives & Durham, 1970; Sarup & Fridland, 1987; Kierdaszuk & Eriksson, 1990; Bohman et al., unpublished results). To describe this type of enzyme kinetics, two Michaelis–Menten equations for two separate ranges of substrate concentrations, with two sets of K_m and V_{max} values, were used. Alternatively, the Hill equation was also used for the entire substrate concentration range, giving a Hill coefficient below 1. The molecular mechanism of these phenomena is not known. In this investigation, we used the phosphate acceptors dCyd, dAdo, and dUrd, the phosphate donor dTTP, the feedback inhibitor dCTP, and the nonsubstrate inhibitor CHAPS, and studied their interaction with enzyme in binary and ternary complexes. The fluorescence spectra of dCyd kinase were quenched by increasing concentration of ligands up to a saturation level, and this effect could be used to measure enzyme–ligand binding.

Enzyme fluorescence was measured at 20 °C for dCyd kinase in buffer C (Materials and Methods), in the absence and presence of ligands. Increasing concentrations of ligands led to decreased fluorescence of dCyd kinase with no change of the peaks for excitation and emission. The quenching pattern was the same at different excitation wavelengths in

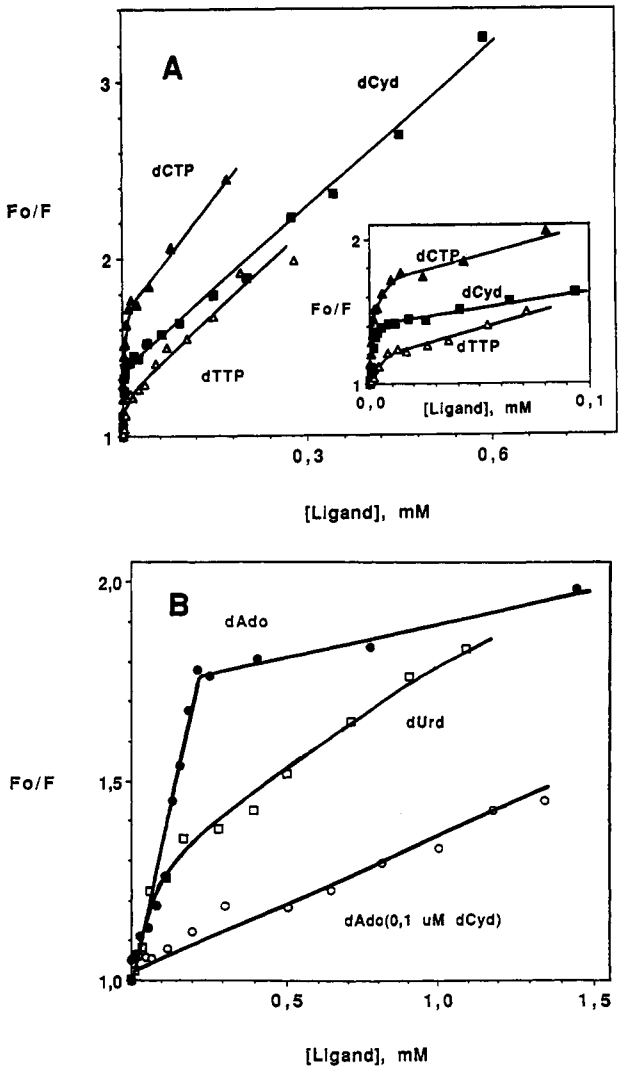

FIGURE 3: Steady-state quenching of dCyd kinase fluorescence by dCyd (■), dCTP (▲) and dTTP (△) (A) and by dAdo (●), dAdo in the presence of 0.1 μM dCyd (○), and dUrd (□) (B). Fluorescence was measured by using buffer C as described under Materials and Methods. It is expressed as the fraction of unquenched fluorescence, F_0, at 290-nm excitation and 332-nm emission wavelengths and plotted as a function of ligand concentration. The insert shows the same data at the low concentration range of ligands.

the range 270–295 nm. The Stern–Volmer plots for fluorescence quenching by dCTP, dCyd, and dTTP (Figures 3A and 5A) and by dAdo (Figures 3B and 5B) were bimodal with transition at about 20, 50, 30, and 180 μM dCTP, dCyd, dTTP, and dAdo, respectively. Thus, enzyme fluorescence quenching can be divided into two processes with different quenching constants and different accessibilities to each quencher. Nonlinear regression analysis has revealed that eq 1–3 (Materials and Methods) did not fit the experimental points obtained from the quenching of the steady-state fluorescence of dCyd kinase. Furthermore, we did not obtain a good fit to eq 4 for the entire range of fluorescence quenching by dCTP, dTTP, Cyd, and dAdo with any single set of parameters (K_{SV},f_a). Parameters obtained from a satisfactory fit at the low concentration range of ligands did not give a good fit at the high concentration range and vice versa. Consequently, two regions of the fluorescence quenching data, indicated as "low" and "high", were analyzed separately, and the results of the best fits are presented in Table I.

The two concentration ranges corresponding to "strong" and "week" quenching are discriminated by approximately

Table I: Stern–Volmer Constants (K_{SV}, f_a) Obtained from Fits of the Modified Stern–Volmer Equation to Enzyme Fluorescence Quenching Data[a]

ligand	concn range (μM)	K_{SV} (μM^{-1})	f_a
dCTP	0–10	2.2 ± 0.2	0.45 ± 0.01
	25–200	0.09 ± 0.03	0.69 ± 0.05
dCyd	0–20	0.78 ± 0.13	0.36 ± 0.02
	90–600	0.009 ± 0.001	0.91 ± 0.04
dTTP	0–25	0.17 ± 0.04	0.30 ± 0.04
	35–280	0.015 ± 0.002	0.74 ± 0.04
dAdo	0–150	0.028 ± 0.009	0.25 ± 0.03
	200–1200	0.0025 ± 0.0003	0.73 ± 0.03
dA/dC	0–1400	0.0019 ± 0.0004	0.54 ± 0.05
dUrd	0–1000	0.0047 ± 0.0007	0.75 ± 0.05

[a] Titrations were made at 20 °C in buffer C (Materials and Methods). Due to the very bad fits of one equation to the entire range of fluorescence quenching by dCTP, dCyd, dTTP, and dAdo, two Stern–Volmer equations were fitted independently for the two ranges of ligand concentration, as indicated. Stern–Volmer quenching constant (K_{SV}, μM^{-1}) and fractional accessibility (f_a) were determined by nonlinear least-squares fits of eq 4, as described under Materials and Methods.

20, 50, 30, and 180 μM dCTP, dCyd, dTTP, and dAdo, respectively. The Stern–Volmer constants as well as accessibilities for the "low" concentration range are highest for dCTP, and they are decreasing in the following order: dCTP > dCyd > dTTP > dAdo. The relations between Stern–Volmer constants (dCTP > dAdo > dTTP > dCyd) and accessibilities (dCyd > dAdo = dTTP = dCTP) for the "high" concentration range are different and show that dCTP is the strongest quencher for both ranges, but the relation between dCyd and dAdo quenching depends on the concentration range of ligand (Table I).

Bimodal fluorescence quenching was not observed with dUrd and with dAdo in the presence of the competitive inhibitor dCyd at 0.1 μM (Figures 3B and 5B), and good fits were obtained with a model of one set of emitter(s) and eq 4 in the concentration range form 0.0 to 1.5 mM (Table I, see also below).

Effect of dCyd and CHAPS on dAdo Quenching. The accessibility of dCyd kinase fluorescence to dAdo quenching was studied in the absence and in the presence of dCyd or the detergent CHAPS, i.e., a substrate and a nonsubstrate inhibitor (Kierdaszuk & Eriksson, 1990). Enzyme fluorescence followed unimodal quenching in the presence of 0.1 μM dCyd, which corresponds to the K_i value for dCyd used as an inhibitor of dAdo phosphorylation (Bohman & Eriksson, 1988). It was not quenched at all during titration with dAdo in the presence of 8 mM CHAPS (Figure 4), which leads to a complete inhibition of dAdo phosphorylation (Kierdaszuk & Eriksson, 1990). This indicates that there is the same binding site for dAdo, dCyd, and CHAPS. The presence of dCyd not only led to different Stern–Volmer constants (Table I) but also changed the overall quenching pattern. The nonlinear plots of F_0/F or $F_0/(F_0-F)$ as a function of dAdo concentration or reciprocal dAdo concentration (Figures 3B and 5B) changed to linear plots in the presence of 0.1 μM dCyd. The fluorescence quenching analysis revealed that the best fit for the dAdo quenching pattern in the presence 0.1 μM dCyd (Figure 5B) was obtained with a modified Stern–Volmer eq 4, giving a Stern–Volmer constant and accessibility equal to 0.0019 ± 0.0004 and 0.54 ± 0.05, respectively.

It is worth noting that the Stern–Volmer constant in the presence of 0.1 μM dCyd is equal to that obtained for the "high" concentration range of dAdo in the absence of dCyd, but maximal accessibility of the binding site to dAdo is lower in the presence than in the absence of dCyd (Table I). Thus,

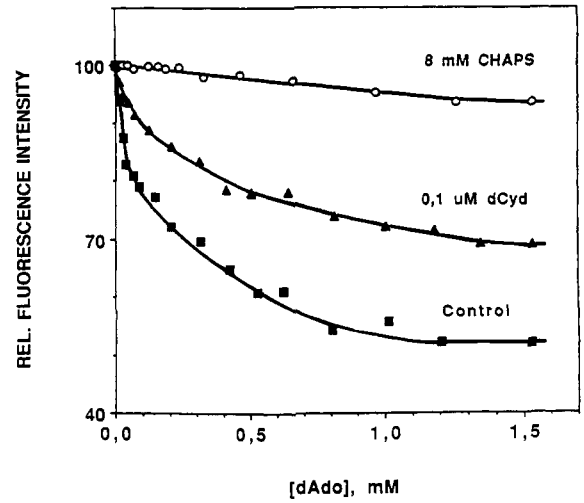

FIGURE 4: Effect of 0.1 μM dCyd and 8 mM CHAPS on dAdo quenching of dCyd kinase fluorescence measured and expressed as indicated for Figure 3.

as measured by this technique, interaction between dCyd kinase and dAdo as well as changes in enzyme conformation accompanying formation of the dAdo–enzyme complex is greatly affected by dCyd and CHAPS, indicating that they all bind to the same site.

Interaction between dCyd Kinase and Ligands. The results of enzyme–ligand binding, calculated from the fluorometric titration of enzyme with dCTP, dCyd, dTTP, dUrd, and dAdo in the absence and presence of 0.1 μM dCyd (see Materials and Methods), are shown as Scatchard plots in Figure 6A,B. They are nonlinear for binding of dCTP, dCyd, dTTP, and dAdo and linear for binding of dUrd, and dAdo in the presence of 0.1 μM dCyd. Nonlinear regression fitting of different models of ligand binding, e.g., with one, two, or three binding sites or states of the enzyme (for discussion, see below), gave a best fit with a two-site (or two-state) model (eq 9; Materials and Methods) for dCTP, dCyd, dTTP, and dAdo binding and with a one-site (or one-state) model for dUrd binding, and dAdo binding in the presence of 0.1 μM dCyd (Table II). We prefer the term state in this presentation for the reasons outlined below. There is apparently a high-affinity state of the enzyme with association constants in the range 0.05–4.5 μM^{-1} and a binding capacity between 0.2 and 0.6. Furthermore, there is a low-affinity state with approximately 10–10^3-fold lower association constants and with a binding capacity of about 1 for dCyd, dTTP, and dAdo (Table II) and 0.6 ± 0.2 for dCTP (Table II). The total binding capacity at saturating concentrations of ligands, based on protein determination (Materials and Methods), is equal to one ligand molecule bound per one molecule of 61-kDa dimer.

Binding of dAdo to dCyd kinase was dramatically changed in the presence of 0.1 μM dCyd, i.e., from bimodal to unimodal (similar to dUrd binding). The dAdo binding constant in the presence of dCyd (0.0019 ± 0.004) was in the same range as its binding constant for the low-affinity state of the enzyme in the absence of dCyd (0.0083 ± 0.0022) and lower than the dUrd binding constant (0.0047 ± 0.0009) (Table II).

The affinity of the ligands to the high-affinity state of the enzyme was highest for dCTP and decreased in the order dCTP > dCyd > dTTP > dAdo, which was also true for the binding capacities. The low-affinity state binds ligands generally more weakly than the high-affinity state and showed highest affinity for dAdo and lowest for dCyd (Table II).

Time-Resolved Fluorescence and Fluorescence Anisotropy of dCyd Kinase and Its Complex with dCyd. Fluorescence

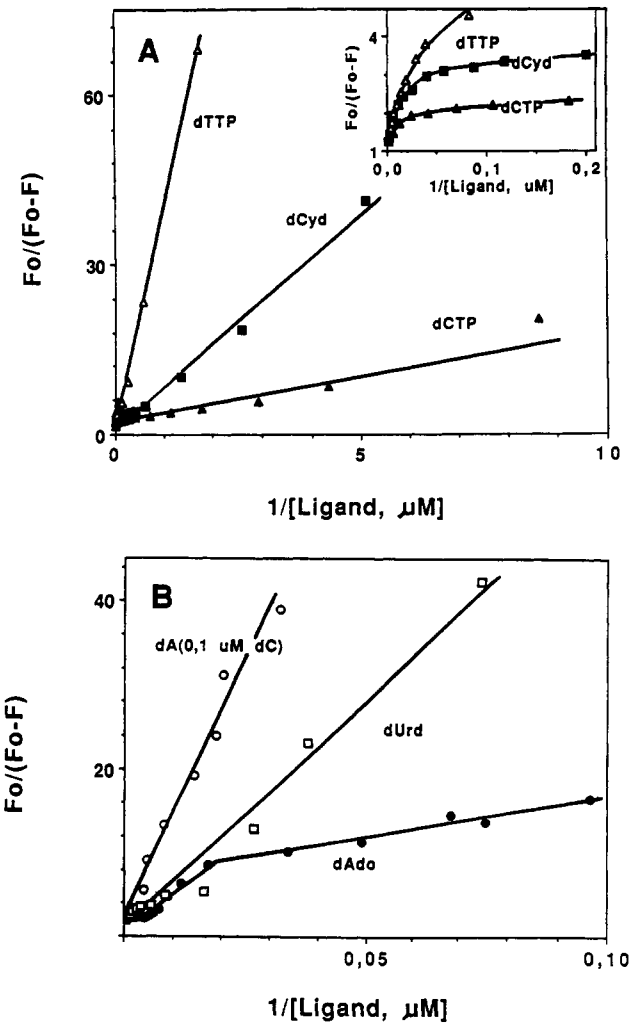

FIGURE 5: Modified Stern–Volmer plot of the steady-state quenching of dCyd kinase fluorescence by dCyd (■), dCTP (▲), and dTTP (△) (a) and by dAdo (●), dAdo in the presence 0.1 μM dCyd (○), and dUrd (□) (B). The decrease of fluorescence ($F_0 - F$) at 290-nm excitation and 332-nm emission wavelengths is expressed as a fraction of the unquenched fluorescence F_0 and plotted as a function of the reciprocal ligand concentration. The insert shows the same data at the high concentration range of ligands. Experimental data are the same as in Figure 3.

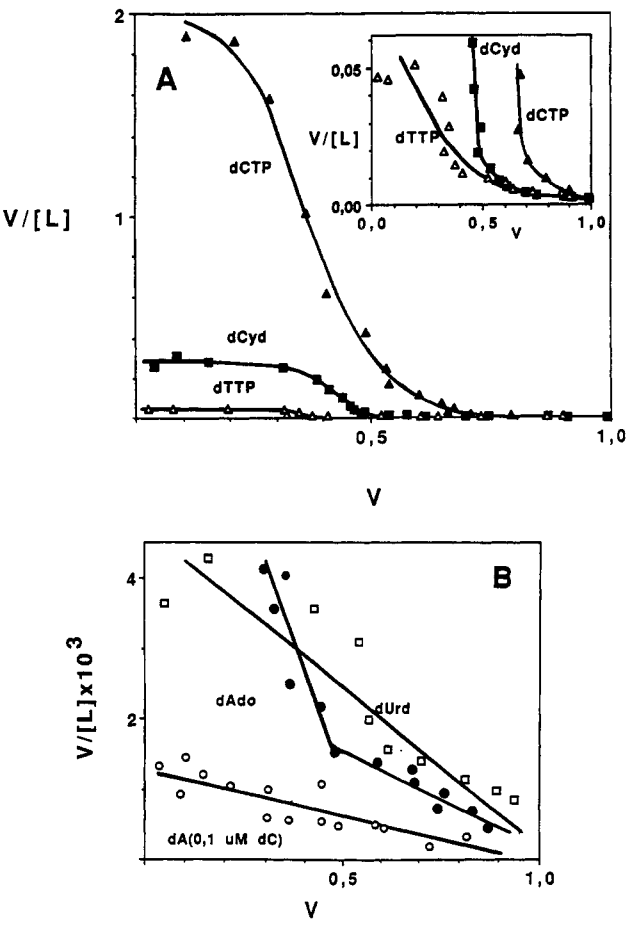

FIGURE 6: Scatchard plot of the binding of dCyd kinase with dCyd (■), dCTP (▲), and dTTP (△) (A) and with dAdo (●), dAdo in the presence of 0.1 μM dCyd (○), and dUrd (□) (B). The concentration of free ligand ([L]) and the number of moles of bound ligand per mole of dCyd kinase and per molar concentration of free ligand (V/[L]) were calculated as described under Materials and Methods. Experimental data are the same as in Figure 3.

and fluorescence anisotropy decays of 4 μM dCyd kinase in buffer C (Materials and Methods), in the absence and presence of dCyd, were measured using a high-resolution photon counting system [Materials and Methods; see also Rigler et al. (1985) and Claesens and Rigler (1986) for details]. The experimantal data were fitted using a sum of varying numbers of exponentials and a nonlinear least-squares fitting procedure (Marquardt, 1963). The quality of fittings was evaluated by structures observed in residuals plots and by the reduced χ^2 values (Nordlund et al., 1989).

Decays of dCyd kinase fluorescence were nonexponential in the absence as well as in the presence of dCyd as illustrated by a representative fluorescence decay curve in Figure 7A. The sum of four exponential terms was required to get good fits to decay curves over a range of 37 ns. The methods of measurement and analysis used here allow us to make good fits of the sum of four exponentials to the fluorescence decay data. This is based on extensive studies of thioredoxin by using a time-correlated single photon counting system with an excitation pulse from a laser system and/or synchrotron, and two methods of analysis: nonlinear least-squares method and maximum entropy method (Merola et al., 1989; Elofsson et al., 1991).

Table II: Computer-Generated Best-Fit Values for the Binding of Ligand to dCyd Kinase at 20 °C in 0.2 M Potassium Phosphate Buffer (pH 7.6) Containing 5 mM $MgCl_2$, 20% Glycerol, and 1 mM DTT[a]

	H-state		L-state	
ligand	N_1	K_1 (μM^{-1})	N_2	K_2 (μM^{-1})
dCTP	0.56 ± 0.02	4.5 ± 0.6	0.6 ± 0.2	0.0041 ± 0.0013
dCyd	0.40 ± 0.02	1.2 ± 0.2	1.0 ± 0.1	0.0023 ± 0.0006
dTTP	0.31 ± 0.05	0.29 ± 0.06	1.2 ± 0.2	0.0041 ± 0.0013
dAdo	0.23 ± 0.04	0.057 ± 0.013	1.3 ± 0.2	0.0083 ± 0.0022
dA/dC			1.0 ± 0.1	0.0019 ± 0.0004
dUrd			1.02 ± 0.07	0.0047 ± 0.0009

[a] The number of moles of bound ligand per mole of dCyd kinase (V) as a function of the concentration of the free ligand ([L]) was obtained from the fluorescence quenching data as described under Materials and Methods. One-, two-, and three- state models of enzyme were fitted to them, and the best fit was obtained using a two-state model with different association constants (K_1, K_2) and different binding capacities (N_1, N_2) (see eq 9 under Materials and Methods). We prefer the term state for the reasons outlined under Results and Discussion.

The results obtained from the fittings (Table III) show that interaction with dCyd affected mainly the amplitudes of the decay terms. After addition of 10.3 μM dCyd, amplitudes I_1 and I_2 decreased from 0.042 ± 0.004 and 0.34 ± 0.007 to 0.032 ± 0.003 and 0.241 ± 0.017, respectively, with a

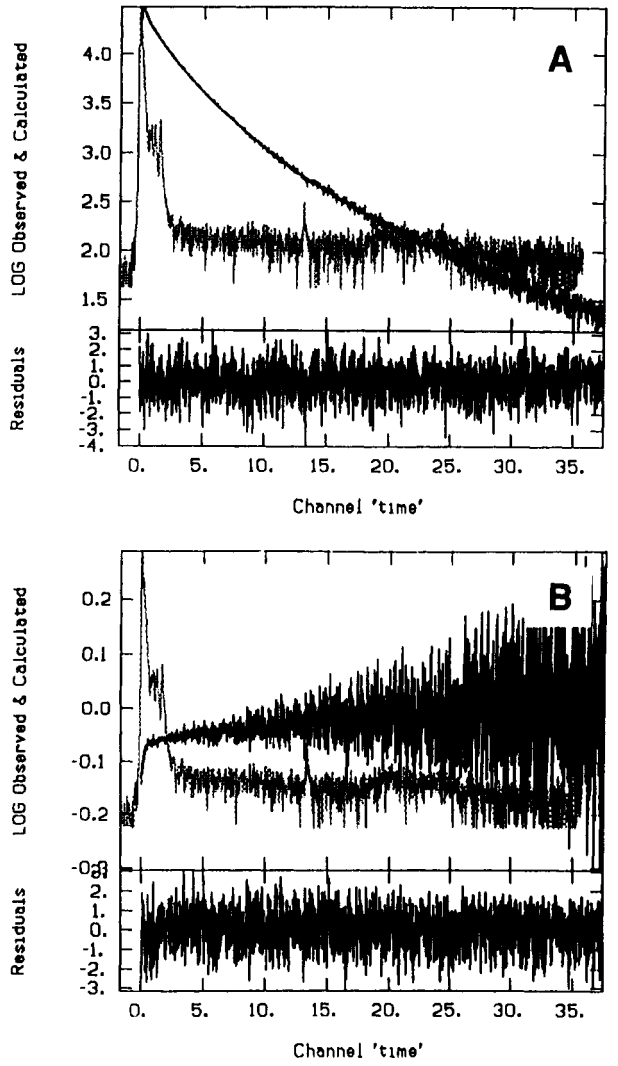

FIGURE 7: Fluorescence decay (A) and fluorescence anisotropy vs time (B) plots of the human dCyd kinase at 20 °C in buffer C (Materials and Methods). The dotted and solid curves represent the profile of the excitation pulse at 295 nm and the fitted theoretical lines of four exponential terms for fluorescence decay and two terms for fluorescence anisotropy decay, respectively. Anisotropy fits were done by starting at the time corresponding to the peak of the excitation pulse.

Table III: Effect of dCyd on the Fluorescence Decay Parameters Obtained from Four-Exponential Fits of the Time-Resolved Fluorescence of Human dCyd Kinase[a]

	dCyd concn (μM)		
	0.0	0.5	10.3
χ^2	1.00	1.05	1.09
I_1	0.042 ± 0.004	0.039 ± 0.006	0.032 ± 0.003
τ_1 (ns)	8.0 ± 0.2	8.2 ± 0.3	8.7 ± 0.3
I_2	0.345 ± 0.007	0.282 ± 0.025	0.241 ± 0.017
τ_2 (ns)	3.1 ± 0.1	3.4 ± 0.2	3.2 ± 0.2
I_3	0.31 ± 0.02	0.35 ± 0.02	0.36 ± 0.02
τ_3 (ns)	1.22 ± 0.09	1.5 ± 0.1	1.27 ± 0.07
I_4	0.30 ± 0.02	0.33 ± 0.01	0.37 ± 0.01
τ_4 (ns)	0.25 ± 0.02	0.33 ± 0.01	0.26 ± 0.02

[a] Standard deviation values represent the 95% confidence intervals.

concomitant increase of I_3 and I_4 (Table III). The lifetime of only one of these components slightly increased on interaction with 10.3 mM dCyd with a change from 8.0 ± 0.2 to 8.7 ± 0.3 ns. Thus, time-resolved decays of dCyd kinase fluorescence demonstrated that the interaction with dCyd led to static quenching of three excited states of its fluorophores

Table IV: Effect of dCyd on the Anisotropy Amplitudes and Decay Times Obtained from Two-Exponential Fits to the Fluorescence Anisotropy Decays of Human dCyd Kinase[a]

[dCyd] (μM)	r_1	ϕ_1 (ns)	r_2	ϕ_2 (ns)	χ^2
0.0	0.179 ± 0.003	28.3 ± 2.3	0.098 ± 0.015	0.18 ± 0.04	0.99
0.5	0.177 ± 0.003	30.4 ± 3.1	0.070 ± 0.011	0.29 ± 0.08	1.04
10.3	0.178 ± 0.003	25.6 ± 2.5	0.079 ± 0.012	0.26 ± 0.07	1.07

[a] Anisotropy fits were done by starting at the time point corresponding to the excitation pulse. Standard deviation values represent the 95% confidence intervals.

(I_i, τ_i; i = 2, 3, 4 in Table III) and to the dynamic quenching of one excited state (I_1, τ_1 in Table III).

Fluorescence anisotropy signals for all samples were well resolved and decayed to zero within a few nanoseconds (Figure 7B). The observed maximum of anisotropy was between 0.25 ± 0.02 and 0.28 ± 0.02. Best fits to the anisotropy decay data were obtained using the sum of two exponential terms with the assumption that there is no association between anisotropy and fluorescence decay components. The value for the initial anisotropy of dCyd kinase in the absence of ligands was found from these fits and was equal to 0.26 ± 0.02. Two sets of values for anisotropy amplitudes (r) and rotational correlation times (ϕ) were obtained from these fits (Table IV). One set, with a low value of the rotational correlation time, was presumably due to the localized micromotion of the tryptophan residues themselves, while another set, with a 100-fold higher value of the rotational correlation time, represents the rotational motion of the entire enzyme molecule. The amplitude corresponding to the longer correlation time is 0.178 ± 0.003, indicating that 68% of the time-dependent decay of anisotropy arises from the motion of the entire protein. The longer correlation time in the absence of dCyd is 28.3 ± 2.3 ns, which is in the range expected for a spherical 61-kDa protein. There is thus no indication of a domain rotation within the enzyme molecule. Interaction with dCyd does not affect the anisotropy decay (Table IV) and indicates that there is no higher order of oligomerization upon enzyme–ligand interaction. Formation of enzyme aggregates was also excluded by FPLC size-exclusion chromatography on the Superose 12 column (Materials and Methods) in the absence and presence of 10 μM dCyd (data not shown). Thus, human dCyd kinase appears to be a rigid protein, and the interaction with dCyd did not affect the motions of its tryptophan residues (Table IV). This must be related to the distance between dCyd, sitting at the active site, and tryptophan residues being the fluorescence probes of enzyme structure. It suggests that dCyd did not interact directly with tryptophans and long-distance interactions between them and/or ligand-induced conformational changes are responsible for the enzyme fluorescence quenching.

This study demonstrates that human dCyd kinase exhibits bimodal binding of the substrates dCyd, dTTP, and dAdo and the feedback inhibitor dCTP, and thus establishes that the complex kinetic properties of this enzyme most likely are due to the direct binding interactions occurring between the enzyme and its ligands. Our binding results further imply that there must be more than one site per enzyme molecule, i.e., one site with high affinity and one with low affinity for the ligands. Although we cannot at present exclude a model with two independent sites of this type, our results show a stoichiometry of binding equal to approximately one ligand per dimer. Furthermore, the time-resolved fluorescence measurements did not indicate any heterogeneity of the excited states of the

enzyme at different ligand concentrations, which makes this hypothesis less likely.

In analogy with structural models of other kinase enzymes (Anderson et al., 1979), we suggest that dCyd kinase can adopt (at least) two different basic states (or conformations) with high and low affinity for the ligands, respectively. With increasing concentration of ligands, the enzyme may be shifted to the low-affinity state, characterized by association constants 10–10^2-fold lower than the high-affinity state. However, structural and direct binding studies are needed to clarify the molecular mechanism for the kinetic and binding properties of dCyd kinase.

It is worth noticing that the relation between the affinities of dCyd and dAdo to dCyd kinase (dCyd > dAdo) is consistent with the relations observed for their substrate efficacies (Eriksson et al., 1991a; Bohman & Eriksson, 1988) and apparent inhibition constants (Bohman & Eriksson, 1988). On the other hand, our results show that the relation between ligand affinities depends on the concentration range of ligands and, together with foregoing, may explain the effect of the concentration range of substrate and/or inhibitor, used in the kinetic experiments, on the inhibition pattern and inhibition constant observed by Ives and Durham (1970).

We earlier suggested that dCyd kinase may exist in two different conformational states: one form responsible for the phosphorylation of cytosine nucleosides and another form able to phosphorylate purine nucleosides (Bohman & Eriksson, 1988). This model is not consistent with the results presented here, because the enzyme in both states, as observed by enzyme fluorescence quenching, binds both ligands, but with different affinities. Thus, the results obtained here suggest that the enzyme in both conformational states should be able to phosphorylate both substrates but with different efficacy and apparent inhibition constants, and the relationship between enzyme efficacies and inhibition constants may depend on the substrate concentration range, i.e., on the conformational state of enzyme. This may also affect the metabolic activation of antiviral and cytostatic agents by dCyd kinase, one of the key enzymes responsible for their phosphorylation. Therefore, detailed knowledge of the substrate-induced specificity and regulation of this enzyme could be important for rational drug design.

REFERENCES

Anderson, C. M., Zucker, S. H., & Steitz, T. A. (1979) *Science 204*, 375–380.

Bohman, C., & Eriksson, S. (1988) *Biochemistry 27*, 4258–4265.

Bradford, M. M. (1976) *Anal. Biochem. 72*, 248–254.

Cheng, Y. C., Domin, B. & Lee, L.-S. (1977) *Biochim. Biophys. Acta 481*, 481–492.

Chottiner, E. G., Shewach, D. S., Datta, N. S., Ashcraft, E., Gribbin, D., Ginsburg, D., Fox, I. H., & Mitchell, B. S. (1991) *Proc. Natl. Acad. Sci. U.S.A. 88*, 1531–1535.

Claesens, F., & Rigler, R. (1986) *Eur. Biophys. J. 13*, 331–342.

Coleman, N., Stroller, R. G., Drake, J. C., & Chamber, B. A. (1975) *Blood 46*, 791–803.

Datta, N. S., Shewach, D. S., Hurley, M. C., Mitchell, B. S., & Fox, I. H. (1989) *Biochemistry 28*, 114–123.

Durham, J. P., & Ives, D. H. (1970a) *Mol. Pharmacol. 5*, 358–375.

Durham, J. P., & Ives, D. H. (1970b) *J. Biol. Chem. 45*, 2276–2284.

Eftink, M. R., & Ghiron, C. A. (1981) *Anal. Biochem. 114*, 199–227.

Ehrenberg, M., Cronvall, E., & Rigler, R. (1971) *FEBS Lett. 18*, 199–203.

Elofsson, A., Rigler, R., Nilsson, L., Roslund, J., Krause, G., & Holmgren, A. (1991) *Biochemistry 30*, 9648–9656.

Eriksson, S., Kierdaszuk, B., Munch-Petersen, B., Oberg, B., & Johansson, N. G. (1991a) *Biochem. Biophys. Res. Commun. 176*, 586–592.

Eriksson, S., Cederlund, E., Bergman, T., Jornwall, H., & Bohman, C. (1991b) *FEBS Lett. 280*, 363–366.

Huang, S. H., Tomic, J. M., Wu, H., Jong, A., & Holcenberg, J. (1989) *J. Biol. Chem. 264*, 14762–14768.

Hurley, M. C., Palella, T., & Fox, I. H. (1983) *J. Biol. Chem. 257*, 6380–6386.

Ives, D. H., & Durham, J. P. (1970) *J. Biol. Chem. 245*, 2285–2294.

Kazai, Y., & Sugino, Y. (1971) *Cancer Res. 31*, 1376–1382.

Kessel, D. (1968) *J. Biol. Chem. 243*, 4739–4744.

Kierdaszuk, B., & Eriksson, S. (1990) *Biochemistry 29*, 4109–4114.

Kierdaszuk, B., Bohman, C., Ullman, B., & Eriksson, S. (1992) *Biochem. Pharmacol. 43*, 197–206.

Kim, M.-Y., Ikeda, S., & Ives, D. H. (1988) *Biochem. Biophys. Res. Commun. 156*, 92–97.

Klotz, I. M., & Hunston, D. L. (1971) *Biochemistry 10*, 3065–3069.

Krenitsky, T. A., Tuttle, J. V., Koszalka, G. W., Chen, I. S., Beacham, L. M., III, Rideout, J. L., & Elion, G. B. (1976) *J. Biol. Chem. 251*, 4055–4061.

Lakowicz, J. R. (1983) *Principles of Fluorescence Spectroscopy*, Plenum, New York.

Leatherbarrow, R. J. (1987) *Enzfitter: A Non-linear Regression Data Analysis Program for the IBM PC*, Elsevier Science Publishers, BV, The Netherlands.

Leatherbarrow, R. J. (1990) *Trends Biochem. Sci. (Pers. Ed.) 15*, 455–458.

Lehrer, S. S. (1971) *Biochemistry 10*, 3254–3263.

Lehrer, S. S., & Leavis, P. C. (1978) *Methods Enzymol. 104*, 441–447.

Marquardt, D. W. (1963) *J. Soc. Ind. Appl. Math. 11*, 431–441.

Merola, F., Rigler, R., Holmgren, A., & Brochon, J.-C. (1989) *Biochemistry 28*, 3383–3398.

Merril, C. R., Goldman, D., & van Keuren, M. L. (1984) *Methods Enzymol. 104*, 441–447.

Meyers, M. B., & Kreis, W. (1976) *Arch. Biochem. Biophys. 177*, 10–15.

Meyers, M. B., & Kreis, W. (1978) *Cancer Res. 38*, 1105–1112.

Momparler, R. L., & Fischer, G. A. (1968) *J. Biol. Chem. 243*, 4298–4304.

Nordlund, T. M., Andersson, S., Nilsson, L., & Rigler, R. (1989) *Biochemistry 28*, 9095–9103.

O'Farrel, P. H. (1975) *J. Biol. Chem. 250*, 4007–4021.

Rigler, R., Claesens, F., & Kristensen, O. (1985) *Anal. Instrum. 14*, 525–546.

Rigler, R., Roslund, J., & Forsen, S. (1989) *Eur. J. Biochem. 188*, 541–545.

Sarup, J. C., & Fridland, A. (1987) *Biochemistry 26*, 590–597.

Scatchard, G. (1949) *Ann. N.Y. Acad. Sci. 51*, 660–672.

Tanford, C. (1968) *Adv. Protein Chem. 23*, 121–282.